

ASCA OBSERVATIONS OF TYPE 2 SEYFERT GALAXIES. II. THE IMPORTANCE OF X-RAY SCATTERING AND REFLECTION

T. J. TURNER,^{1,2} I. M. GEORGE,^{1,2} K. NANDRA,^{1,3} AND R. F. MUSHOTZKY¹

Received 1997 March 20; accepted 1997 May 22

ABSTRACT

We discuss the importance of X-ray scattering and Compton reflection in type 2 Seyfert Galaxies, based upon the analysis of *ASCA* observations of 25 such sources. Consideration of the iron $K\alpha$ complex, $[O\ III]$ line, and X-ray variability suggest that NGC 1068, NGC 4945, NGC 2992, Mrk 3, Mrk 463E, and Mrk 273 are dominated by reprocessed X-rays. We examine the properties of these sources in more detail.

We find that the iron $K\alpha$ complex contains significant contributions from neutral and high-ionization species of iron. Compton reflection, hot gas and starburst emission all appear to make significant contributions to the observed X-ray spectra.

Mrk 3 is the only source in this subsample that does not have a significant starburst contamination. The *ASCA* spectrum below 3 keV is dominated by hot scattering gas with $U_X \sim 5$, $N_H \sim 4 \times 10^{23} \text{ cm}^{-2}$. This material is more highly ionized than the zone of material comprising the warm absorber seen in Seyfert 1 galaxies, but may contain a contribution from shock-heated gas associated with the jet. Estimates of the X-ray scattering fraction cover 0.02%–5%. The spectrum above 3 keV appears to be dominated by a Compton reflection component, although there is evidence that the primary continuum component becomes visible close to ~ 10 keV.

Subject headings: galaxies: active — galaxies: nuclei — line: formation — X-rays: galaxies

1. INTRODUCTION

The optical spectra of most nearby active galactic nuclei (AGNs) are dominated by narrow optical lines (e.g., Lawrence 1991) and are therefore broadly classified as type 2 Seyfert galaxies. However, broad optical lines with characteristics similar to those observed in Seyfert 1 galaxies were discovered in the polarized light from NGC 1068 (Antonucci & Miller 1985). It was suggested that the polarization arose as a result of electron scattering, implying that the optical broad line region in NGC 1068 is only visible in scattered light. When several more examples of the phenomenon were found (Miller & Goodrich 1990) a general model emerged in which the nuclear spectra of both Seyfert types 1 and 2 are the same, but the nuclear regions of type 1 are observed directly, while Seyfert 2 nuclei are hidden behind a large column of obscuring material. The simplest geometry for the obscuring material is a torus. This allows orientation-dependant obscuration, and hence, can explain the existence of the type 1 and type 2 Seyfert galaxies. *Hubble Space Telescope* (*HST*) observations have now resolved a torus in the AGN NGC 4261 (Ferrarese, Ford, & Jaffe 1996). Such a torus allows the existence of some lines of sight for which radiation from within the torus can only be viewed via scattering. The high opacity of the obscuring material makes it difficult to observe the central engines of Seyfert 2 galaxies directly at most wavelengths. Medium energy X-rays can penetrate column densities of up to $\sim 10^{24} \text{ cm}^{-2}$, allowing a direct view of some type 2 nuclei, but observations of sources with even larger columns should reveal predominantly scattered or reflected X-rays below 10 keV.

In a companion paper (Turner et al. 1997a, hereafter Paper I) we presented the data analysis results of *ASCA* observations of a sample of 17 Seyfert 2 galaxies, plus eight narrow emission line galaxies (NELGs). Paper I dealt with temporal and spectral X-ray results from those two classes of AGNs together. The observations were drawn from the public archive, and the sources do not comprise a complete sample. The data selection, reduction, and analysis are described in detail in Nandra et al. (1997, hereafter N97) and Paper I. The sources in which we observe the nucleus through the absorber will be discussed in another paper (Turner et al. 1997b). In the present paper we determine which sources from the original sample are most likely to be dominated by reprocessed X-ray emission, and we then examine the properties of this subset in detail.

2. SIGNATURES OF REPROCESSED X-RAY EMISSION

Iron $K\alpha$ lines in AGNs arise via reprocessing of the primary X-rays. If $K\alpha$ lines of very high equivalent width are observed, this is an indication that one is viewing a spectrum dominated by reprocessing. For Seyfert 2 galaxies, it is appropriate to consider two types of reprocessing, which we shall refer to as “Compton reflection” and “scattering.” We use the term Compton reflection (or simply “reflection”) to mean reprocessing of X-rays via Compton scattering and fluorescence by material that is optically thick to electron scattering. We use the term “scattering” to apply to the case where the optical depth to electron scattering is $0 < \tau < 1$.

In Seyfert 1 galaxies, the iron $K\alpha$ lines are thought to arise via Compton reflection from an accretion disk (e.g., N97), which produces lines of equivalent width \sim few hundred eV with respect to the directly observed continuum (e.g., George & Fabian 1991). However, the equivalent width of the iron $K\alpha$ line can be as high as a few keV with respect to the Compton-reflected continuum (George &

¹ Laboratory for High Energy Astrophysics, Code 660, NASA/Goddard Space Flight Center, Greenbelt, MD 20771.

² Universities Space Research Association.

³ NAS/NRC Research Associate.

Fabian 1991; Matt, Perola, & Piro 1991). Such a situation is somewhat unlikely in the case of an accretion disk, since the central continuum and iron line are both produced in a very small region and obscuring one without the other would require an unusual geometry. However, the reflection may also occur at the inner surface of the obscuring material, possibly the torus, and the orientation and opening angle can then allow a view of the inner surface, but not the illuminating source. Some early *ASCA* results showed that Compton reflection of nuclear radiation from optically thick material can be an important component of Seyfert 2 galaxies. The Circinus galaxy (Matt, Brandt, & Fabian 1996) and NGC 6552 (Fukazawa et al. 1994) show strong reflection components dominating the spectra even below 10 keV.

If the iron $K\alpha$ line is produced in optically thin gas then its observed equivalent width can also be large as long as the direct continuum is not observed. The line equivalent width is a strong function of the ionization state of the material (which is also the case for the reflected iron lines, but both the disk and torus are thought to be relatively neutral). For low ionization states the equivalent width of the iron K shell line, measured against the scattered nuclear emission (plus free-free and bound-free emission from the scattering gas), can be as high as ~ 1 keV for the 6.4 keV line (Netzer 1996) and could appear to be up to a few keV for an iron line blend.

Although it is tempting to interpret lines of high equivalent width as evidence for a dominant reflected or scattered

component, high equivalent widths can also arise if the ionizing radiation is anisotropic (e.g., Ghisellini et al. 1991) or if there is a significant lag between a fall in the continuum flux and the reprocessed spectrum. Indeed, Weaver et al. (1996) suggested a 16 year lag between a drop in continuum and line fluxes to explain the large equivalent width in the iron $K\alpha$ line for NGC 2992 at the *ASCA* epoch. Thus, when assessing whether or not a source is dominated by reprocessing, it is important to take other evidence into account.

An alternative method of determining whether a type 2 Seyfert galaxy contains a hidden X-ray source is by examining the flux in the $[O\ III]\ \lambda 5007$ emission line (hereafter simply referred to as $[O\ III]$) observed in the optical regime. Mulchaey et al. (1994) found a strong correlation between $[O\ III]$ and hard X-ray flux in a sample of Seyfert 1 galaxies. This provides an independent estimate of the nuclear X-ray luminosity for Seyfert 2 galaxies for comparison with the observed X-ray luminosity. If the observed X-ray luminosity is substantially less than that predicted by $[O\ III]$, this is an indication that the X-ray emission is being observed indirectly, with only a fraction of the total luminosity reaching our line of sight.

3. IDENTIFICATION OF THE REFLECTED/SCATTERED SOURCES

A summary of the *ASCA* sample is detailed in Table 1. We now consider the properties of these sources in relation to the above discussion, to determine which Seyfert 2 galaxies are likely to be dominated by reprocessed emission.

TABLE 1
THE *ASCA* SEYFERT 2 SAMPLE

| Name (1) | R. A. ^a (2) | Decl. ^a (3) | z^a (4) | Class ^a (5) | L_X (6) | $L_{[O\ III]}$ (7) |
|-----------------------|---------------------------|---------------------------|--------------|---------------------------|--------------------|-----------------------|
| MCG-01-01-043 | 00 10 03.5 | -04 42 18 | 0.0300 | S2 | 42.88 | ... |
| NGC 526A | 01 23 55.1 | -35 04 04 | 0.0192 | NELG ^b | 43.77 | 43.49 |
| NGC 1068 | 02 42 40.8 | -00 00 47 | 0.0038 | S2 ^b | 41.15 | 45.10 |
| NGC 1667 | 04 48 37.2 | -06 19 12 | 0.0152 | S2 | 40.46 | 44.37 |
| E0449-184 | 04 51 38.8 | -18 18 55 | 0.338 | S2 | 44.86 | ... |
| NGC 1808 | 05 07 42.3 | -37 30 46 | 0.0033 | SB/S2 | 40.62 | 43.00 |
| NGC 2110 | 05 52 11.4 | -07 27 22 | 0.0076 | NELG | 42.82 | 43.94 |
| Mrk 3 | 06 15 36.3 | 71 02 15 | 0.0135 | S2 ^b | 42.33 | 45.44 |
| NGC 2992 | 09 45 41.9 | -14 19 35 | 0.0077 | NELG ^b | 42.05 | 44.46 |
| MCG-5-23-16 | 09 47 40.2 | -30 56 54 | 0.0083 | NELG ^b | 43.43 | 44.14 |
| NGC 4507 | 12 35 36.5 | -39 54 31 | 0.0118 | S2 | 42.28 | 44.43 |
| NGC 4945 | 13 05 26.2 | -49 28 16 | 0.0019 | S2 | 40.53 | ... |
| NGC 4968 | 13 07 06 | -23 40 43 | 0.0100 | S2 | 42.45 | 44.83 |
| NGC 5135 | 13 25 44 | -29 50 01 | 0.0137 | S2 | 43.16 | 44.76 |
| NGC 5252 | 13 38 15.9 | 04 32 33 | 0.0230 | S1.9 | 43.24 | 43.88 |
| Mrk 273 | 13 44 42.1 | 55 53 13 | 0.0378 | S2 | 42.45 | 45.69 |
| Mrk 463E | 13 56 02.9 | 18 22 19 | 0.0500 | S2 | ^b 42.75 | 44.75 |
| NGC 5695 | 14 37 22.0 | 36 34 04 | 0.0141 | S2 | <40 | 42.65 |
| NGC 6251 | 16 32 31.9 | 82 32 17 | 0.0230 | S2 | 42.50 | 44.30 |
| NGC 6240-49 | 16 52 59.3 | 02 23 59 | 0.0245 | S2 | 43.61 | 46.17 |
| ESO 103-G35 | 18 38 20.2 | -65 25 42 | 0.0133 | S2/NELG | 43.14 | 43.92 |
| IC 5063 | 20 52 02.9 | -57 04 14 | 0.0113 | S2 ^c | 43.15 | 44.42 |
| NGC 7172 | 22 02 02.1 | -31 52 12 | 0.0086 | S2/NELG ^b | 43.22 | ... |
| NGC 7314 | 22 35 45.7 | -26 03 03 | 0.0047 | S1.9/NELG | 42.59 | 44.40 |
| NGC 7582 | 23 18 23.2 | -42 22 11 | 0.0053 | S2/NELG ^d | 42.32 | 43.64 |

NOTES.—Group C sources are boldface. Col. (1), name; cols. (2) and (3), right ascension (hours, minutes, and seconds) and declination (degrees, arcminutes, and arcseconds), J2000; col. (4), redshift; col. (5), Seyfert type—SB = starburst galaxy, NELG = narrow emission line galaxy; col. (6), log of observed 2–10 keV luminosity in ergs s^{-1} (absorption corrected, but see § 4.1); col. (7), log of intrinsic 2–10 keV luminosity inferred from dereddened $[O\ III]$ fluxes, in ergs s^{-1} .

^a From the NASA Extragalactic Database (NED).

^b Polarized broad lines have been detected: Tran 1995a, 1995b.

^c Polarized broad lines have been detected: Inglis et al. 1997.

^d Polarized broad lines have been detected: Heisler et al. 1997.

which the hard X-ray flux is just the scattered X-rays. For that reason, we use the more tightly determined correlation for the Seyfert 1 galaxies as the basis of our calculation. The resulting intrinsic luminosities are tabulated and plotted against the observed values (from Paper I, Table 12) in Figure 2.

Unfortunately, the [O III] flux can include some unresolved contribution from starburst emission, depending on the aperture used and the level and location of starburst activity in the host. We might expect some predicted luminosities to be too high because of this confusion. We also expect scatter in the plot due to variability and the imperfect nature of the correlation between [O III] and hard X-ray luminosity. Given these uncertainties we highlight (by naming the sources on the plot) only those sources whose predicted luminosities exceed the observed by a factor of more than 100. This confirms the suggestion of a hidden X-ray continuum in NGC 1068, Mrk 3, and NGC 2992, which we had already concluded based on the iron line evidence. The lack of an [O III] flux measurement for NGC 4945 excludes that source from this test. However, heavy obscuration in NGC 4945 is well established. Done et al. (1996) used the combined *Ginga*, *ASCA* and *OSSE* data to confirm the Iwasawa et al. (1994) result that the nucleus of NGC 4945 is so heavily absorbed that the direct component is only visible above 10 keV.

Examination of the [O III] flux also indicates a hidden X-ray continuum in Mrk 273, Mrk 463E, NGC 4507, NGC 1667, NGC 1808, NGC 4968, and NGC 5695. The cases for reprocessing in Mrk 273 and Mrk 463E now become much stronger, since the iron $K\alpha$ lines also had a very high equivalent width (although the constraints were such that an alternative origin could not be ruled out). The iron $K\alpha$ equivalent widths indicate consistency with an origin in the line-of-sight absorber in NGC 4507, NGC 1808, NGC 4968, and NGC 1667 (although the latter two are highly

uncertain). Thus, we conclude that the evidence for extensive reprocessing in these cases is inconclusive, and we do not consider them in detail in this paper. NGC 5695 has no observed *ASCA* flux (just an upper limit) and so it is not plotted in Figure 2. However, if the intrinsic luminosity implied by the [O III] flux was observed directly, NGC 5695 would have been detected easily by *ASCA*. This suggests that the absorbing column exceeds a few 10^{24} cm^{-2} . Elongated narrow-line regions in some Seyfert galaxies appear to be ionized by a more intense radiation field than is directly observable, (e.g., Haniff, Wilson, & Ward 1988; Pogge 1988; Tadhunter & Tsvetanov 1989). This provides supporting evidence for hidden nuclei in sources such as Mrk 3.

3.3. X-Ray Variability

Of the sources most likely to be dominated by reprocessed emission, only NGC 1068 was bright enough for us to search for rapid X-ray variability (Paper I). It did not vary significantly when sampled on a 128 s timescale. While several of the sources appear to show hard X-ray variability on timescales of years (Polletta et al. 1996), all cases except Mrk 3 are based upon comparison between *HEAO/A1* and *ASCA* or *Ginga*. The low angular resolution of *HEAO/A1* yields systematically high fluxes assigned to those measurements of many source fluxes in the Polletta et al. (1996) catalog. Thus, we do not consider apparent flux variations that depend on the *HEAO/A1* measurements, to be reliable.

NGC 2992 is unique amongst the reprocessing-dominated sources because it shows correlated variability in the hard and soft X-ray regimes down to timescales of a few days (Weaver et al. 1996; Turner & Pounds 1989). This indicates that we are seeing the 0.5–10 keV flux directly. Thus, Weaver et al. (1996) suggest that NGC 2992 has a strong observed iron $K\alpha$ line because of a lag between direct and reprocessed flux, rather than due to obscuration of the nucleus. However, the 6.4 keV line is still inferred to arise by Compton reflection, and so we continue to include it in our consideration of the reprocessed source spectra.

Thus, taking the iron $K\alpha$, [O III] line and variability evidence together, we are most confident that the *ASCA* observations are dominated by reprocessed X-rays in the cases of NGC 1068, NGC 4945, NGC 2992, Mrk 3, Mrk 463E, and Mrk 273. For ease of reference we now denote these as “group C” sources and these are marked with squares on Figure 1. For later reference we denote the sources lying on the Leahy and Creighton line to be “group A,” and those with iron $K\alpha$ equivalent widths lying between that line and 230 eV to be “group B.” Group B sources have iron $K\alpha$ lines consistent with those observed from the relativistic accretion disk in Seyfert 1 galaxies (N97). The properties of group A and B sources will be discussed in a later paper (Turner et al. 1997b). We continue here by investigating what the X-ray properties of group C sources can tell us about conditions in the reprocessing media.

4. THE NATURE OF THE REPROCESSING REGIONS

4.1. Constraints from Absorption

The absorbing columns detected in the reprocessed sources ($\sim 10^{22} \text{ cm}^{-2}$) do not necessarily represent the line-of-sight attenuation to the nucleus. Rather, they may represent opacity in the scattering gas. In principle, then, measurements of that absorption could be used to indicate

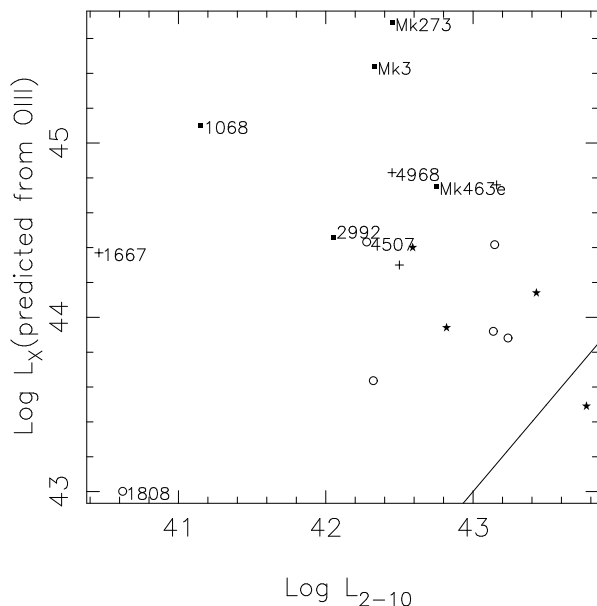


FIG. 2.—Predicted intrinsic 2–10 keV luminosity, based upon the [O III] line flux (see text for details) vs. the observed (absorption-corrected) luminosity. We have annotated those sources having predicted luminosities more than a factor of 100 greater than the observed values. Again, group A sources are marked as circles, group B sources as stars, and group C sources as squares (§ 3.3).

the column density and ionization state of that medium. However, misleading spectral fitted parameters can be obtained when fitting simple continuum models (Paper I) to spectra dominated by photoionized emission. To illustrate this point, Figure 3 shows a typical emission spectrum from ionized absorbing gas observed in the line of sight to $\geq 60\%$ of Seyfert 1 galaxies (Reynolds 1997; George et al. 1997). The gas has an ionization parameter $U_X \sim 0.125$ and column $N_H \sim 4 \times 10^{22} \text{ cm}^{-2}$, based on the analysis of *ASCA* observations of Seyfert 1 galaxies (see George et al. 1997 for details and the definition of U_X). For a demonstration we simulated a 40 ks *ASCA* observation of the emission spectrum of the warm absorber gas and then fitted the simulated spectrum with a model composed of an absorbed power law plus a Raymond-Smith equilibrium plasma. We find a best-fitting spectrum with a flat power law of $\Gamma = 0.87$ absorbed by a column $N_H = 1.8 \times 10^{22} \text{ cm}^{-2}$ plus an unabsorbed plasma with $kT = 0.86 \text{ keV}$, with a fitted statistic of $\chi^2 = 424/331$. Both the fitted parameters and acceptability are reminiscent of values obtained when fitting some Seyfert 2 galaxies with simple models (e.g., Paper I). Apparently, the presence of the emission spectrum from the scattering gas can mimic an absorbed flat power law plus a soft thermal component.

If the warm absorber commonly seen in Seyfert 1 galaxies is the same material that scatters nuclear X-rays into our line of sight in the Seyfert 2 case, then we should expect the same distribution of ionization parameter and column for these components, and we discuss this in § 6, in the context of the spectral results from Mrk 3. Krolik & Kriss (1995) suggest that an X-ray heated wind can produce both the warm absorber in Seyfert 1 galaxies, and warm scattering gas affording a view of the central nuclei of Seyfert 2 galaxies. The wind idea is supported by the blueshifts observed in the UV absorption systems in some QSOs and Seyfert galaxies. Those systems generally show blueshifts indicative of outflow velocities of a few hundred km/s. Observations to date of the X-ray absorber have been insensitive to such small velocity shifts (George et al. 1997). In any case, veloc-

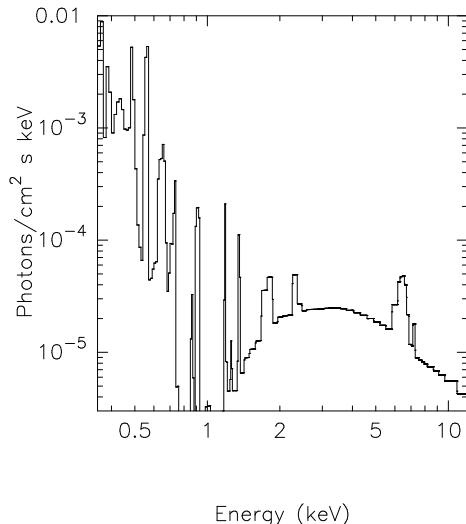


FIG. 3.—Emission spectrum from a warm absorber including scattered continuum emission (from a $\Gamma = 2$ power law) plus thermal and line emission from the hot gas. The gas has an ionization parameter $U_X \sim 0.12$ and column $N_H \sim 4 \times 10^{22} \text{ cm}^{-2}$, based on the analysis of *ASCA* observations of Seyfert 1 galaxies (see George et al. 1997).

ity shifts might be most difficult to observe in type 2 Seyferts because the wind velocity vector could be almost perpendicular to our line of sight.

4.2. Constraints from Emission

The strength of the iron $K\alpha$ lines in the group C sources is a strong indication that they arise via reprocessing. As stated above, the majority of the line emission occurs close to 6.4 keV, suggesting an origin via reflection from the absorbing material. This component of the line profile is expected to be free of the relativistic effects evident in the iron $K\alpha$ line profiles of Seyfert 1 galaxies (N97). Figure 4 shows the individual ratios in the iron $K\alpha$ regime, from reprocessed sources with the most significant iron lines, i.e., NGC 1068, Mrk 3, NGC 2992 and NGC 4945. Ratios are shown for the summed SIS plus GIS data, and the SIS data alone. The SIS data alone have superior energy resolution, but unfortunately our systematic method of analysis has left few significant SIS data bins at high energies. We note that Iwasawa, Fabian, & Matt (1996) obtained a clearer SIS line profile for NGC 1068 by optimizing the data screening for that observation (the conservative criteria used in N97 and Paper I yield a low SIS exposure compared to the on-time of the observation in this case).

The SIS data can provide some useful information when the data/model ratios are co-added. The energy scale of each SIS spectrum was redshift corrected to the rest frame of the source and then the average SIS instrument ratio was calculated utilizing all of the group C sources (vs. the best continuum model in each case, from Paper I). Figure 5 shows the result of this summation. The average SIS data/model ratio is shown, and the dotted Gaussian profile represents the SIS instrument response for a narrow line observed at a rest energy of 6.4 keV. This plot does not show the actual line profile, rather the counts ratio compared to the best continuum model (to get the true profile you have to multiply the ratio plot by the continuum form). Excess flux is evident blueward and redward of 6.4 keV. The former seems most likely to indicate the presence of high-ionization species of iron $K\alpha$, which are present in NGC 1068, Mrk 3, NGC 4945, and NGC 2992 when tested on an individual basis (Paper I). Mrk 463E and Mrk 273 did not have sufficient signal-to-noise to detect features of a similar relative strength. All of the sources showed a significantly broad line when the iron $K\alpha$ regime was modeled with a single Gaussian, so the sources either have multiple unresolved components, like NGC 1068 (Marshall et al. 1993), or the iron $K\alpha$ lines are broadened.

It therefore seems most likely that the spectra contain contributions both from Compton reflection and the scattering gas, although as noted above, if the latter has multiple ionization states and the dominant one is relatively cool, this could account for a strong 6.4 keV component without the need for reflection. Of particular interest in this regard is the observation of a red wing to the line. This signature—which amounts to $\sim 10\%$ of the core flux—is not expected to be produced by scattering from an optically thin medium. The same feature is observed with the same equivalent width in the iron $K\alpha$ profile of Seyfert 1 galaxies (N97). Iwasawa et al. (1997) noted the presence of a red wing in the iron $K\alpha$ line profile of NGC 1068. Those authors noted that it was consistent with the “Compton shoulder” expected from downscattering of 6.4 keV photons in a reflecting medium. The Mrk 3 and NGC 4945 profiles appear to show

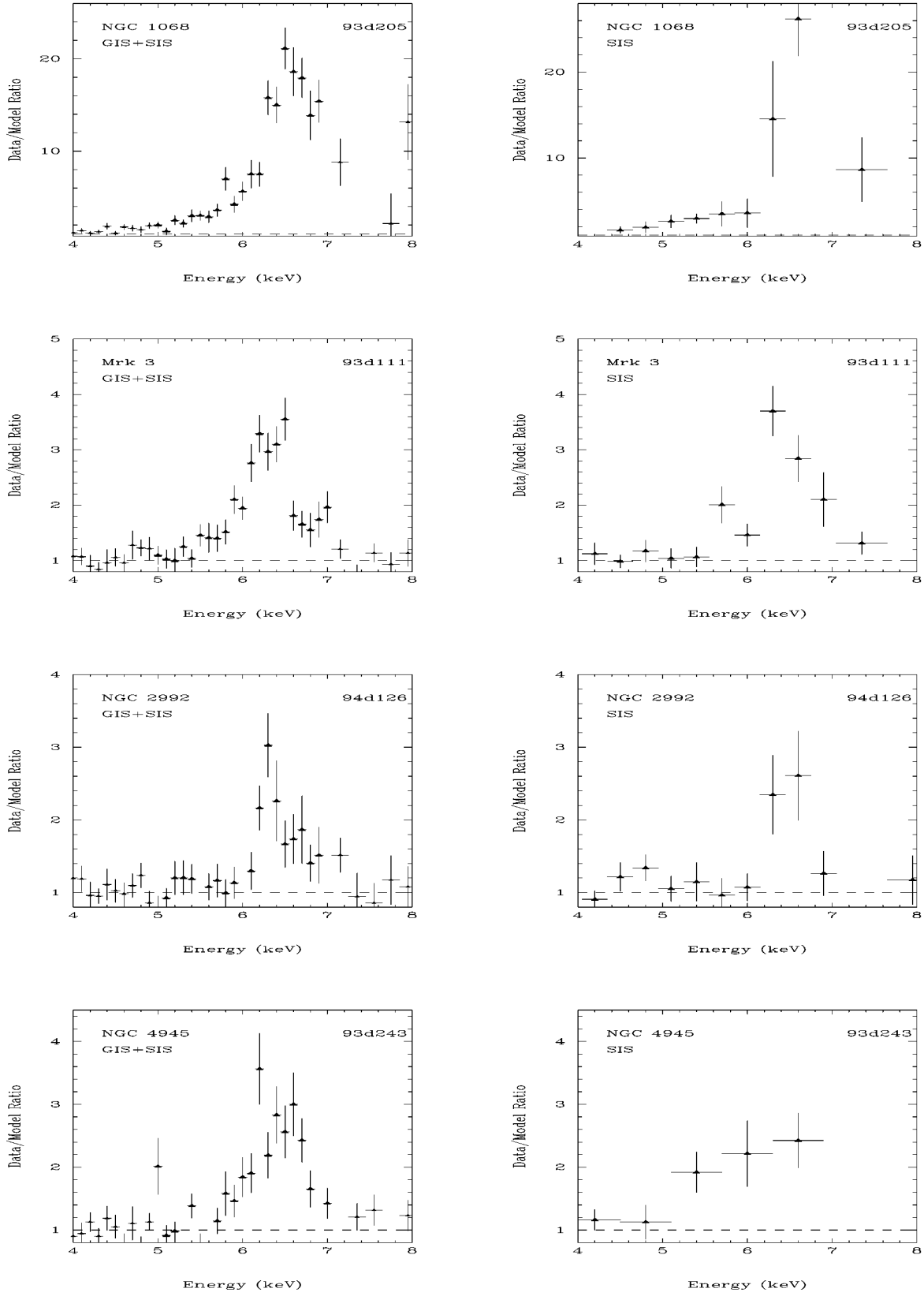


FIG. 4.—Data/model ratios vs. the best-fit simple continuum model for NGC 1068, Mrk 3, NGC 2992, and NGC 4945 (from Paper I). The X-axis shows the observed frame energy. In the left hand panels data from all four instruments have been combined for clarity. In the right hand panels, the two SIS data sets have been combined. An excess of counts is generally evident in the 5–7 keV data, vs. the continuum model. This indicates the presence of strong iron K shell emission lines in most objects.

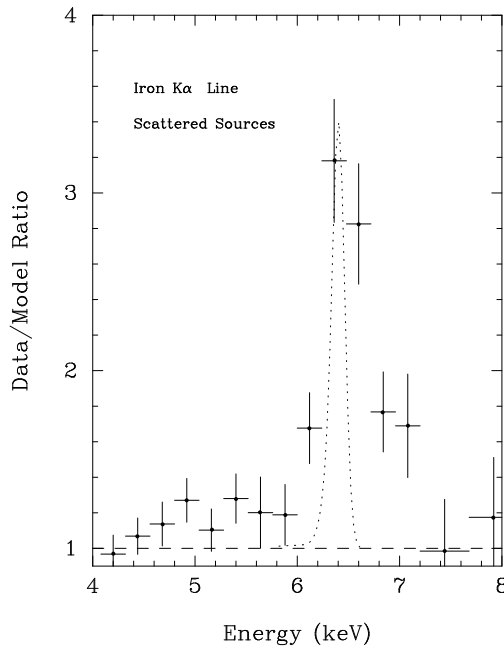


FIG. 5.—Average data/model ratio in the iron $K\alpha$ regime. The group C data sets were used to create the mean ratio. Each data set was corrected to the rest frame energy before the objects were combined and so the X-axis shows the rest frame energy. The dotted Gaussian profile represents the SIS instrument response for a narrow line observed at a rest energy of 6.4 keV.

the same effect but NGC 2992 does not (Fig. 4, although the data do not allow us to place interesting constraints in this respect, Mrk 463E and Mrk 273 are inconclusive due to a lack of signal-to-noise in the 5–7 keV regime). Iwasawa et al. (1997) state that the red wing in NGC 1068 is more likely to be attributed to a Compton shoulder than to the relativistic effects observed in Seyfert 1 galaxies, since the contribution of the relativistic disk should be observed only in scattered light. However, if the continuum is also scattered, the relativistic disk component would have the same equivalent width with respect to that continuum as it does when it is directly observed. This would result in a red wing similar to that observed. The fact that some of the line profiles extend to energies lower than could easily be produced by Compton scattering in a cold medium suggests that the red wings may indeed be associated with the relativistic disk component seen in scattered light. However, uncertainties in the continuum modeling used to produce the line profiles may make such a conclusion premature.

The presence of the high-ionization lines make the average line profile from group C significantly different to that obtained for a sample of Seyfert 1 galaxies (N97) (which shows a strong broad red wing but no high-ionization species of iron $K\alpha$). While the two types of Seyfert galaxy may well contain iron $K\alpha$ line components from all the same regions the high-ionization lines would be swamped by the direct continuum in the Seyfert 1 case.

If these high-ionization iron K shell lines arise in the scattering gas, then in the model of Heisler, Lumsden, & Bailey (1997), we might expect to preferentially detect these species in sources for which a hidden BLR has been detected in the scattered optical light. This is because their model places the scattering region within the obscuring torus, so hidden BLRs are visible when sources are observed from lines of sight that skim the edge of the torus,

i.e., for a narrow range of observing angles. For sources viewed at a favorable angle the torus hides the central engine and BLR, but allows direct observation of the scattering gas. For sources viewed more edge-on, the scattering region is also hidden. Our data are consistent with that idea, in that we detect these line species in all the sources where we see the BLR in scattered optical light and for which we have sufficient signal-to-noise ratio in the X-ray spectra to tell.

We would expect to observe emission lines other than iron K from the scattering gas, particularly at soft X-ray energies, and indeed many such lines are observed (Paper I). Ideally, then, one would wish to compare detailed photoionization models for the scattering region with our data to determine the physical characteristics of the gas. However, some ambiguity remains as to whether the observed soft X-ray lines arise via nuclear processes or are related to starburst activity. Furthermore, high-ionization iron K species are detected in sources such as NGC 5135, which has a strong starburst component. This raises the question as to whether some of the iron $K\alpha$ emission might arise from non-nuclear processes. Clearly, separating the emission of the Seyfert from that of the starburst is necessary for a conclusive answer.

5. STARBURST CONTRIBUTIONS TO THE X-RAY FLUX

Starburst emission is a well-documented phenomenon in many Seyfert 2 galaxies. It is not yet clearly established as to whether starburst activity occurs at the same level in Seyfert 1 galaxies. Some studies indicate a similar star formation rate in Seyfert 1 galaxies and starburst galaxies (Yamada 1994), while others indicate that the host galaxies of type-2 nuclei have significantly higher levels of starburst activity than type 1 nuclei (Maiolino et al. 1995). If it does occur at the same level in the two types of Seyfert, the X-ray emission associated with the starburst would be swamped by the Seyfert 1 nuclei. For a sample of obscured AGNs, we would expect some observable differences as the degree of nuclear obscuration varies between sources, and hence, the contrast is changed between contributions from the host galaxy versus the nucleus. In Paper I we found that in the 0.5–4.5 keV band the estimated average contribution from starbursts in the host galaxy was $\sim 60\%$ for the Seyfert 2 galaxies, versus 2% for the NELGs. We also noted that soft X-ray lines were observed in many Seyfert 2 galaxies, but in none of the NELGs (Paper I). As strong soft X-ray lines are seen in some starburst galaxies (Ptak et al. 1997), these facts necessitate careful consideration of the starburst contribution to the X-ray flux.

Unfortunately, the *ASCA* data do not allow us to spatially deconvolve the X-ray lines produced by starburst activity from those produced in the scattering gas. However, Wilson et al. (1992) find that the starburst disk in NGC 1068 can provide a 2–10 keV flux of $\sim 2-8 \times 10^{-12}$ erg cm^{-2} s^{-1} , consistent with all of the *ASCA* flux. So, although the high equivalent widths and energies of the iron $K\alpha$ lines link them with reflection or scattering of nuclear radiation, some or all of the other X-ray emission lines may be attributable to starburst activity.

Examining the level of starburst “contamination” for targets in group C, we find just one source that is not significantly contaminated by a starburst component, Mrk 3 (Paper I and Pogge & De Robertis 1993). This source is particularly interesting as, despite the lack of starburst

emission, it does show significant soft X-ray emission lines. Mrk 3 is one of the brightest Seyfert 2 galaxies with a hidden BLR. Detailed analysis of the optical data has shown the broad lines have a polarization of 20% (Tran 1995b). Although there has been some debate over the Hubble type of the host galaxy for Mrk 3, it is now thought to reside in an elliptical host galaxy (Jenkins 1981; Wagner 1987), and it has a radio jet with knots and a large bright radio lobe (Kukula et al. 1993). This source offers us the best opportunity available to date to obtain information about conditions in the X-ray reprocessing regions of a Seyfert 2 galaxy.

6. A CASE STUDY: MARKARIAN 3

We constructed a spectral model table of the emission spectrum from a slab of photoionized gas illuminated by an ionizing continuum using the ION photoionization code. ION includes the important excitation and ionization processes, full temperature and radiative transfer solutions, while emission, absorption and reflection by the gas are calculated assuming thermal and ionization equilibrium. The model tables we use assume a photon index $\Gamma = 2.0$ in the 0.2–50 keV range, and $\Gamma = 1.5$ from 1.6–40.8 eV. The optical to X-ray energy index is assumed to be $\alpha = 1.5$. Cosmic abundances were used, and a constant density $n_H = 10^{10} \text{ cm}^{-3}$ throughout the slab. The X-ray ionization parameter is defined as

$$U_X = \int_{0.1 \text{ keV}}^{10 \text{ keV}} \frac{Q(E)}{4\pi r^2 n_H c} dE, \quad (1)$$

where $Q(E)$ is the number of photons at energy E and r is the distance from the source to the illuminated gas. For more details of the ION code see Netzer (1993, 1996). The absorption of this component was fixed at the Galactic value $8.7 \times 10^{20} \text{ cm}^{-2}$. In addition to this component we allowed a pure Compton-reflection spectrum utilizing the model of Magdziarz & Zdziarski (1995) plus a Gaussian line (since their reflection model does not include line emission). We assumed reflection of a $\Gamma = 2.0$ continuum (with no exponential cutoff; the data do not allow us to determine whether any cutoff is present) from relatively neutral material (only H and He are ionized) viewed face-on. This model provided a good fit to the data yielding $\chi^2 = 349/328$.

6.1. The Hard X-Ray Spectrum

The energy at which the primary continuum becomes visible depends on the column obscuring it. If the nucleus of Mrk 3 was obscured by a column $\sim 10^{24} \text{ cm}^{-2}$ as observed in NGC 4945, then the direct continuum component should become observable close to $\sim 10 \text{ keV}$. In fact the *ASCA* spectrum does show a small hard tail compared to the Compton-reflection model noted above. The *ASCA* fit improves by $\Delta\chi^2 \sim 11$ on addition of a highly absorbed power-law component of fixed index $\Gamma = 2$. This component is absorbed by a column of $N_H = 1.3^{+2.2}_{-0.6} \times 10^{24} \text{ cm}^{-2}$, and provides 25% of the 5–10 keV observed flux. We estimate the intrinsic (unabsorbed) 2–10 keV luminosity of this nuclear component to be $\sim 10^{43} \text{ erg s}^{-1}$. The reflecting medium is implied to subtend $\Omega \sim 2 \pm 1\pi$ steradians to the intrinsic continuum source. This model is shown in Figure 6, along with the data/model ratio.

Iwasawa et al. (1994) find a different solution to the *ASCA* spectral data, with a model in which the direct

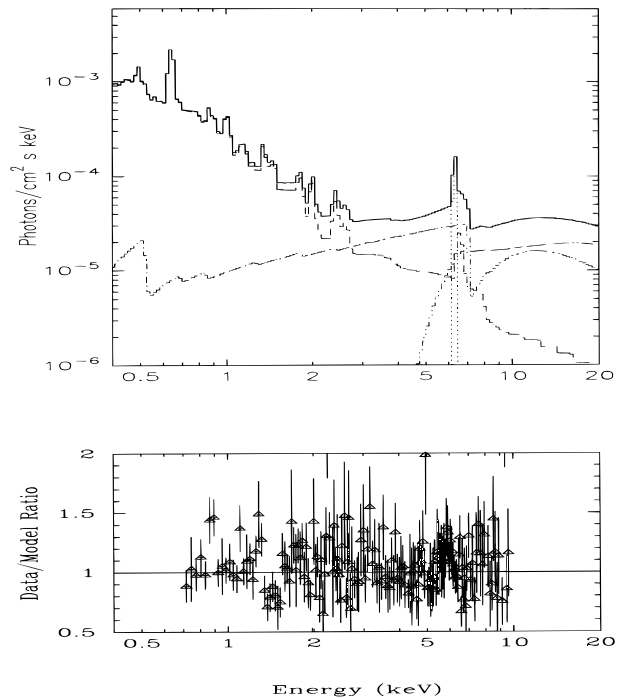


FIG. 6.—Best-fit model to the *ASCA* spectral data for Mrk 3, along with the data/model ratio. The SIS and GIS ratios have been combined for clarity of illustration. The model comprises an emission spectrum from highly ionized gas, a Compton reflection component and an absorbed power law (see § 6). A Galactic column of $8.7 \times 10^{20} \text{ cm}^{-2}$ covers all components.

absorbed continuum component dominates the 3–10 keV spectrum, absorbed by $N_H \sim 4 \times 10^{23} \text{ cm}^{-2}$. No reflection component is included in their model. However, the observed equivalent width in iron K α is $977^{+193}_{-137} \text{ eV}$ (when modeled as a narrow line; Paper I), which requires a column of 10^{24} cm^{-2} in order for the line to be produced by transmission (Fig. 1), assuming a Leahy & Creighton (1993) geometry. The upper limit on column yielded by the Iwasawa et al. (1994) solution is $5.8 \times 10^{23} \text{ cm}^{-2}$, which is too low to produce the line, assuming the Leahy & Creighton geometry is applicable.

Our model, which includes the Compton-reflection component, yields a better fit by $\Delta\chi^2 = 59$ (obtained by comparing the fit of their model and ours using our data sets). The inclusion of a Compton-reflection component also provides a natural explanation for the very flat $\Gamma = 1.30 \pm 0.3$ spectrum observed in the *Ginga* data (Awaki et al. 1990). The inclusion of the reflection component is the reason we obtain a higher column for the direct component than Iwasawa et al. (1994); in fact our column of $\sim 10^{24} \text{ cm}^{-2}$ is consistent with the strength of the iron K α line. That line is now consistent either with an origin in the line-of-sight material or via Compton reflection alone. The indication that the line flux variations are correlated with the hard X-ray continuum variations favors the latter (see § 6.3).

However, we also note that the simple absorption model we used does not include the effects of Thompson scattering, and so may yield an underestimate of the column in the regime $N_H \sim 10^{24} \text{ cm}^{-2}$. Krolik, Madau, & Zycki (1994), and Ghisellini, Haardt, & Matt (1994) found that transmission of the AGN continuum through a Compton-thick absorber produces a filtration that looks very much

like a Compton reflection component. This is an alternative explanation of the shape of the hard X-ray spectrum.

6.2. The Soft X-Ray Spectrum

The soft part of the spectrum (below ~ 3 keV) is well modeled by the emission from a photoionized plasma with $U_x = 4.8^{+1.5}_{-1.3}$ and $N_H = 3.5^{+1.7}_{-1.4} \times 10^{23} \text{ cm}^{-2}$. This highly ionized gas can produce the 6.96 keV component of the iron line and the Si and S lines and scatters some of the nuclear radiation into our line of sight. This component is much more highly ionized than the zone of material comprising the warm absorber evident in *ASCA* observations of Seyfert 1 galaxies (when a single-zone model is assumed for the latter). The temperature of the gas is $\sim 10^5$ K, consistent with that of the optical scattering gas in NGC 1068 (Miller, Goodrich, & Mathews 1991).

However, this soft X-ray flux might have some contribution from shocked gas. Recent *HST* observations (Capetti et al. 1995) have resolved a subarcsec region of continuum emission, which they propose could either be associated with gas shocked by passage of the jet, or the BLR scattering gas. Those authors also show a $\sim 2''$ S-shaped region of narrow line gas, although this gas is photoionized by the central AGN, it is too cool to produce the soft X-ray emission observed.

The absorption-corrected 2–10 keV luminosity in the ionized-gas component alone is $5 \times 10^{41} \text{ ergs s}^{-1}$. The scattered fraction of flux is proportional to the product of the scattering efficiency and the solid angle of the scattering material. Assuming the scattering gas dominates over shock-heated gas, then our X-ray data indicate a scattered X-ray fraction of $\sim 5\% \pm 1\%$. This is comparable to the few percent generally derived from optical measurements of type 2 AGNs (e.g., Pier et al. 1994). The estimate of intrinsic 2–10 keV luminosity from the dereddened [O III] line flux is $3 \times 10^{45} \text{ ergs s}^{-1}$, yielding an estimate of 0.02% for the scattered fraction. Alternatively, using the Mulchaey (1994) relationship between infrared and hard X-ray luminosity we estimate an intrinsic luminosity of $6.6 \times 10^{43} \text{ ergs s}^{-1}$ and a scattered fraction 0.75%.

6.3. Constraints from Variability

If the hard X-ray emission is transmitted through the obscuring material in our line of sight, then we will observe the hard X-ray variations of the nucleus directly. Alternatively, if the hard X-ray emission is dominated by a reflected component, then the light curve of the reprocessed emission will lag the primary emission and be smoothed. The degree of lag and the smoothing depend on the location and size of the reprocessor and its geometry.

The soft X-ray flux has not varied over the ~ 13 year baseline for which we have flux measurements (Iwasawa et al. 1994), suggesting that it comes from an extended region. If this flux is associated with the $0''.35 \times 1''$ bar of continuum emission resolved by *HST* (Capetti et al. 1995), then it originates in a region several hundred pc in size.

However, the hard X-ray emission of Mrk 3 is variable. The fastest historical change in the hard flux was a factor of 2 drop between the *Ginga* and *BBXRT* observations, taken 1 year apart. The 6.4 keV line flux appears to vary in a way consistent with that change in the continuum while the soft X-ray flux remains steady, ruling out a lag between the reprocessed and nuclear flux as the explanation for the high equivalent width.

The observed variability places a rough constraint on the size of the variable source to be less than 0.3 pc. The shape of the spectrum suggests that the nucleus is not observed directly and therefore this constraint applies to the reprocessing material, rather than the central source. This could have a small scale height; in fact Gallimore et al. (1996) suggest that a pc scale maser disk with toroidal geometry exists in NGC 1068, based on a water maser observation. This disk is observed at high inclination (82°) and can provide sufficient opacity to block the X-ray continuum below 10 keV.

7. DISCUSSION AND CONCLUSIONS

Consideration of the iron $K\alpha$, [O III] line, and X-ray variability indicates that the *ASCA* observations are dominated by reprocessed X-rays in the cases of NGC 1068, NGC 4945, NGC 2992, Mrk 3, Mrk 463E, and Mrk 273.

The iron $K\alpha$ line profiles of these sources show significant contributions from neutral and high-ionization species of iron. Thus, it appears that Compton reflection, the hot scattering gas, and/or starburst emission contribute to the 5–7 keV regime.

Mrk 3 shows negligible starburst contamination, so the X-ray spectrum is probably dominated by processes intimately related to the active nucleus. The *ASCA* spectrum can be described by hot scattering gas in the soft X-ray regime, with $U_x \sim 5$, $N_H \sim 4 \times 10^{23} \text{ cm}^{-2}$. This material is more highly ionized than the zone of material comprising the warm absorber seen in Seyfert 1 galaxies, but it may have some contribution from shock-heated gas associated with the jet. Estimates of the scattering fraction cover 0.02%–5%. The hard X-ray spectrum of this source appears to be dominated by a Compton-reflection component, although there is evidence that the primary continuum component becomes visible close to ~ 10 keV.

It is obvious that a big problem with analysis of X-ray observations of type 2 Seyferts to date has been the inability to deconvolve the starburst emission (and any other extended thermal gas) from that in the immediate environment of the nucleus (and while *ROSAT* provided several arcsecond spatial resolution it offered data over a narrow bandpass with low spectral resolution). *HST* observations have now resolved a $1''$ – $2''$ region in which the UV scattering occurs in NGC 1068 (Antonucci et al. 1994), corresponding to a region ~ 110 – 220 pc in size. The *AXAF* High Resolution Camera (HRC) will allow subarcsecond X-ray imaging. Assuming the UV scattering region is closely related to the X-ray scattering region, then we will be able to spatially resolve the X-ray “mirror” for the first time in NGC 1068 and other nearby sources such as NGC 4945 and NGC 1808, and we will be able to resolve the bar of emission observed in Mrk 3 by *HST*. If the X-ray scattering gas turns out to be the same gas observed as a warm absorber in Seyfert 1 galaxies, then such imaging may map the distribution of the warm absorber. As the starburst emission often extends over regions many tens of arcseconds or larger for nearby AGNs, *AXAF* spectra should allow us to separate the starburst and nuclear components for at least some AGNs. *Beppo SAX* and *XTE* also offer an opportunity to acquire X-ray spectra above 10 keV, which might help us determine the true nature of Mrk 3.

We are grateful to *ASCA* team for their operation of the satellite, to Keith Gendreau for discussions on *ASCA* cali-

bration issues, Hagai Netzer for use of model tables generated using the photoionization code ION, Andy Ptak for comments on the properties of starburst galaxies, and Julian Krolik for useful comments. This research has made use of the SIMBAD database, operated at CDS, Strasbourg, France; of the NASA/IPAC Extragalactic database,

which is operated by the Jet Propulsion Laboratory, Caltech, under contract with NASA; and data obtained through the HEASARC on-line service, provided by NASA/GSFC. We acknowledge the financial support of Universities Space Research Association (I. M. G., T. J. T.) and the National Research Council (K. N.).

REFERENCES

- Antonucci, R., & Miller, J. S. 1985, *ApJ*, 297, 621
 Antonucci, R., Hurt, T., & Miller, J. S. 1994, *ApJ*, 430, 210
 Awaki, H., Koyama, K., Kunieda, H., & Tawara, Y. 1990, *Nature*, 346, 544
 Capetti, A., Macchetto, F., Axon, D. J., Sparks, W. B., & Boksenberg, A. 1995, *ApJ*, 448, 600
 Cardelli, J. A., Clayton, G. C., & Mathis, J. S. 1989, *ApJ*, 345, 245
 Done, C., Madejski, G. M., & Smith, D. 1996, *ApJ*, 463, L63
 Ferrarese, L., Ford, H. C., & Jaffe, W. 1996, 470, 444
 Fukazawa, Y., et al. 1994, *PASJ*, 46, 141
 Gallimore, J. F., Baum, S. A., O'Dea, C. P., Brinks, E., & Pedlar, A. 1996, *ApJ*, 462, 740
 George, I. M., & Fabian, A. C. 1991, *MNRAS*, 249, 352
 George, I. M., Turner, T. J., Netzer, H., Nandra, K., Mushotzky, R. F., & Yaqoob, T. 1997, *ApJS*, submitted
 Ghisellini, G., George, I. M., Fabian, A. C., & Done, C. 1991, *MNRAS*, 248, 14
 Ghisellini, G., Haardt, F., & Matt, G. 1994, *MNRAS*, 267, 743
 Haniff, C. A., Wilson, A. S., & Ward, M. J. 1988, *ApJ*, 334, 104
 Heisler, C. A., Lumsden, S. L., & Bailey, J. A. 1997, *Nature*, 385, 700
 Inglis, M. D., et al. 1997, *MNRAS*, 263, 895
 Iwasawa, K., Fabian, A. C., & Matt, G. 1997, *MNRAS*, 289, 443
 Iwasawa, K., Yaqoob, T., Awaki, H., & Ogasaka, Y. 1994, *PASJ*, 46, L167
 Jenkins, C. R. 1981, *MNRAS*, 197, 829
 Krolik, J. H., & Kriss, G. A. 1995, *ApJ*, 447, 512
 Krolik, J. M., Madau, P., & Zycki, P. 1994, *ApJ*, 420, L57
 Kukula, M. J., Ghosh, T., Pedlar, A., Schilizzi, R. T., Miley, G. K., de Bruyn, A. G., & Saikia, D. J. 1993, *MNRAS*, 264, 893
 Lawrence, A. 1991, *MNRAS*, 252, 586
 Leahy, D. A., & Creighton, J. 1993, *MNRAS*, 263, 314
 Magdziarz, P., & Zdziarski, A. A. 1995, *MNRAS*, 273, 837
 Maiolino, R., & Rieke, G. H. 1995, *ApJ*, 454, 95
 Marshall, F., et al. 1993, *ApJ*, 405, 168
 Matt, G., Brandt, W. N., & Fabian, A. C. 1996, *MNRAS*, 280, 823
 Matt, G., Perola, G. C., & Piro, L. 1991, *A&A*, 247, 25
 Miller, J. S., & Goodrich, R. 1990, *ApJ*, 355, 456
 Miller, J. S., Goodrich, R., & Mathews, W. G. 1991, *ApJ*, 378, 47
 Mulchaey, J. S., Koratkar, A., Ward, M. J., Wilson, A. S., Whittle, M., Antonucci, R. J., Kinney, A., & Hurt, T. 1994, *ApJ*, 436, 586
 Nandra, K., George, I. M., Mushotzky, R. F., Turner, T. J., & Yaqoob, T. 1997, *ApJ*, 477, 602
 Netzer, H. 1993, *ApJ*, 411, 594
 ———. 1996, *ApJ*, 473, 781
 Pier, E. A., Antonucci, R., Hurt, T., Kriss, G., & Krolik, J. 1994, *ApJ*, 428, 124
 Pogge, R. W. 1988, *ApJ*, 328, 519
 Pogge, R. W., & De Robertis, M. M. 1993, *ApJ*, 404, 563
 Polletta, M., Bassani, L., Malaguti, G., Palumbo, G. G. C., & Caroli, E. 1996, *ApJS*, 106, 399
 Ptak, A., Serlemitsos, P., Yaqoob, T., Mushotzky, R. F., & Tsuru, T. 1997, *AJ*, 113, 1286
 Reynolds, C. S. 1997, *MNRAS*, 286, 513
 Tadhunter, C., & Tsvetanov, Z. 1989, *Nature*, 341, 422
 Tran, H. 1995a, *ApJ*, 440, 597
 ———. 1995b, *ApJ*, 440, 574
 Turner, T. J., George, I. M., Nandra, K., & Mushotzky, R. F. 1997a, *ApJS*, 113, in press (Paper I)
 ———. 1997b, *ApJ*, submitted
 Turner, T. J., & Pounds, K. A. 1989, *MNRAS*, 240, 833
 Wagner, S. J. 1987, *A&A*, 185, 77
 Weaver, K. A., Nousek, J., Yaqoob, T., Mushotzky, R. F., Makino, F., & Otani, C. 1996, *ApJ*, 458, 160
 Wilson, A. S., Elvis, M., Lawrence, A., & Bland-Hawthorn, A. 1992, *ApJ*, 391, L75
 Yamada, T. 1994, *ApJ*, 423, L27